34th Annual International Conference of the IEEE EMBS
San Diego, California USA, 28 August - 1 September, 2012

A Cell Counting Method for BEVS Based on Nonlinear Transformed Sliding Band Filter

Kuanquan Wang, *Senior Member, IEEE*, Dong Sui, Wei Wang, Yongfeng Yuan, Wangmeng Zuo, *Member, IEEE*

Abstract— **Insect cell is the host of baculovirus in Baculovirus Expression Vector System (BEVS). However, the insect cell counting is an obstacle that constrains the efficiency in BEVS. In this paper, an insect cell counting method based on Transformed Sliding Band Filter (TSBF) was proposed according to insect cell cultivation manner. The proposed method was then applied to insect cell image datasets, and results exhibited that the average relative error rate was 2.21% compared with manual counting. Growth curve evaluation showed that this method was suitable to the protocol of cell cultivation. These exciting results proved that the proposed method was an ideal automatic counting tool for inset cells in BEVS.**

I. Introduction

BEVS has been widely used to express heterologous genes in various cell lines since the mid-1980s [1]. Insect cell is the host of baculovirus in BEVS and its density is very important for the following experiments and virus preparation. Insect cell counting traditionally was manipulated by human using microscope with counting chambers [2]. But this method is prone to errors by the same or different persons during counting. So it was required to repeat to validate the results [3].

In the 1940s, Wallace Coulter introduced a method to count suspended particles in a fluid, which was a milestone in solving cell counting automatically [2]. Since then, some microscopic image analyzing tools were created for cell counting. Several image filters and segmentation methods were also employed for cell identification and counting in microscopy images, such as counter or region-based, minimum-error-threshold and histogram-based methods. In addition, watershed transform, gray level threshold, morphological operators, and artificial neural network (ANN) were also used for investigating the same problem [4-7]. On the other hand, various tools have been introduced for solving cell counting problems in different images, such as ImageJ and Cellprofiler [8]. But there is no tools suitable for all cell lines because of their differences in shape, size and structure [8, 9, 10].

In this paper, an insect cell counting method for BEVS was proposed. This method was based on a nonlinear filter, Sliding Band Filter (SBF), which was employed for lung nodule detection [11] and fluoresce stained cell nuclei identification in dark field [12, 13]. The SBF filter can detect low contrast cell nuclei and cytoplasm information lost in the background noise and it can also reduce the uncertainty caused by noise. Furthermore, the parameters of the filter are directly related to cell shape and size, leading to an easy setup by biotechnologist who even knows little about image processing technic. In this paper, we evaluated the convergence of gradient vector in the bright field, and transformed the convergence index in SBF filter to fit the location to detect. The result showed the proposed method can be applied to insect cell counting in different infecting stages, and was able to improve the efficiency in the protocol of BEVS.

II. Material and Datasets

A. Host Cells Preparation

There are four type insect cell lines commonly used for BVES application and was listed in Table 1, which support various levels of expression and differential glycosylation with the same recombinant protein [14]. We chose the most widely used cell type *Sf9*, a clonal isolated from the *Spodoptera frugiperda* cell line *IPLB-Sf21-AE*, as the host cells.

TABLE I. Common Used Insect Cell Lines In BEVS

Insect Species	Cell Line
Spodoptera frugiperda	*Sf9*
Spodoptera frugiperda	*Sf-21*
Trichoplusia ni	*Tn-368*
Trichoplusia ni	*High-Five™ BTI-TN-5B1-4*

After recovering from liquid nitrogen, *Sf*9 insect cells was diluted by *SF*900 II complete medium with 10% Fetal bovine serum and 1% double-antibiotic(Penicillin and Streptomycin). Cell suspension with density of 2×10^5 cells/mL was prepared at 27℃ for counting task in different concentrations. After the density reached $2\sim3\times10^6$ cells/mL, the insect cells growth into exponential growth phase, various kinds of experiments was permitted during this period. When its density reached $5\sim6\times10^6$ cells/mL, it came in to stationary phase with no growth of cells and descends.

*Research supported by National Nature Science Foundation of China (NSFC) grant No.61001167, No.61173086 and No.61179009.

Kuanquan Wang (Professor), is with the Biocomputing Research Center, School of Computer Science and Technology, Harbin Institute of Technology, Harbin, China (corresponding author to provide phone: +86-0451-86412871;e-mail: wangkq@hit.edu.cn).

Dong Sui, is with the Biocomputing Research Center, School of Computer Science and Technology, Harbin Institute of Technology, Harbin, China (e-mail: suidong10@gmail.com).

Wei Wang, is with School of Computer Science and Technology, Harbin Institute of Technology, Harbin, China (e-mail: weiwang@gmail.com)

Yongfeng Yuan (Doctor), is with the Biocomputing Research Center, School of Computer Science and Technology, Harbin Institute of Technology, Harbin, China (e-mail: yuanyongfeng@gmail.com)

Wangmeng Zuo (Doctor), is with the Biocomputing Research Center, School of Computer Science and Technology, Harbin Institute of Technology, Harbin, China (e-mail: cswmzuo@gmail.com)

B. Manual Counting Data Collection

Insect cells' density in suspension culture medium usually calculated by Neubauer chambers, for the reason that it includes enough regions to evaluate both low and high concentration of insect cells [2], showed in Figure 1.

Traditionally, the insect cells were diluted at certain ratio using *Sf*900 II medium according to the period of cell cultivation. And then were injected into the chamber where the volume (the depth and area) was standardized. The cell number (Squ_{INC}) from the field was obtained by the visual inspection in 1 mm2 regions in the chamber. Finally, the density of insect cells (Vol_{INC}) was calculated by Eq. 1.

$$Vol_{INC} = Squ_{INC} \times C_{depth} \times Cell_{cct} \quad (1)$$

Where:

C_{depth}: represent the depth of the chamber;

$Cell_{cct}$: represent the concentration of the insect cells.

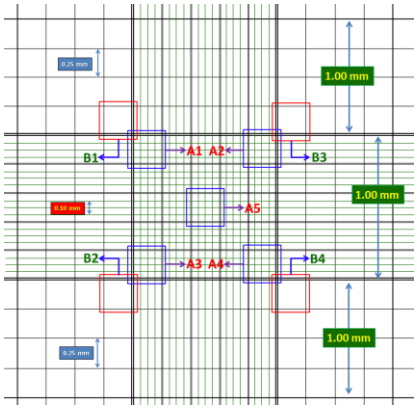

Figure 1. Neubauer Chamber with nine 1×1 mm² squires with 0.1 mm depth. A1 to A5 region are divided in 1/25 mm² regions, and B1 to B4 region are divide in 1/16 mm² regions.

Typically, insect cells visual evaluation is calculated from the 4 or 5 regions. For example, 4 regions are B1, B2, B3, B4, and 5 regions are A1, A2, A3, A4, A5 in figure 3. In this paper, we mainly focused on region A1 to A5.

C. Image Data Sets Acquisition

*Sf*9 insect cells images with resolution of 1280×960 was collected using confocal microscopy with 200×magnification for performing cell counting task. For each 24 hours until cell grow into stationary phase, 3 samples were collected separately and marked sample 1, sample 2 and sample 3 according to the collecting sequence. Microscopic images of region A1 to A5 was collected separately from each sample.

III. Methodology

A. Cell Detector Design Using TSBF

In this paper, we proposed a new method based on Slid Bang Filter (SBF) for insect cells counting using image enhancement for the reason that the SBF filter was employed to enhance certain features on gray level images [13]. Do not like most of the liner filters' small support regions (m×m pixels which m∈ $\{2, 3, 5, \cdots\}$), the SBF filter had a larger one up to 61×61 pixels. This filter was originated from a nonlinear SBF, a member of Convergence Index (CI) family, was used for identifying the density packed cells in another work of our team.

The CI family was design for enhancing the rounded convex region in digital images, and was based on the maximization of CI at each pixel of spatial coordinates(x, y). CI in this paper is defined by the following formulations:

$$CI(x,y) = \frac{1}{N}\sum_{(m_R,n_R)} cos\,\alpha(m_R,n_R) \quad (2)$$

Where (x, y) represent coordinate of interesting pixel, N is the number of pixels of the filter in the support region R, $\alpha(m_R, n_R)$ is the angle between gradient vector in pixel (m_R, n_R) and the line connected (x, y) and (m_R, n_R).

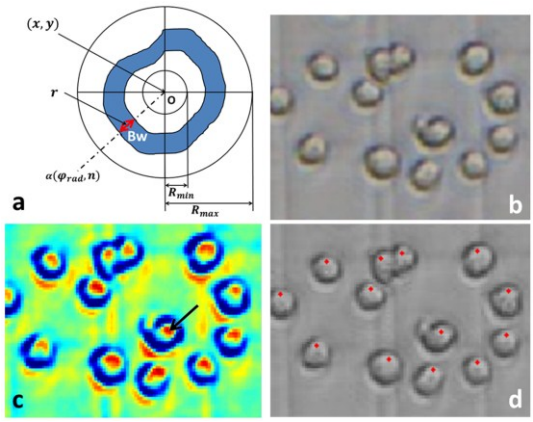

Figure 2. TSBF for cell detection. (a) schematic of the SBF support region; (b) Sf9 insect cells in confocal microscopy; (c) image after filtering by TSBF; (d) cell detected results on the same image using non-maximal suppression.

Several members have been proposed in CI family, such as Coin Filter(CF), Iris Filter(IF), Adaptive Ring Filter(ARF) and the Sliding Band Filter (SBF) [16, 17], differences of these members are the definition of the support region R. The SBF filter has a band with fixed width support region, whose position changed in each radius direction allows maximize the average convergence index in the band width. Figure 2 (a) depicts the scheme of support region in SBF. The SBF filter is defined as:

$$SBF(x,y) = \frac{1}{N}\sum_{rad=1}^{N} \underset{R_{min}<r<R_{max}}{max}\left(\frac{1}{Bw+1}\sum_{r-(Bw/2)}^{r+(Bw/2)} CI(rad,n)\right) \quad (3)$$

With

$$CI(rad,n) = cos(\varphi_{rad} - \alpha(\varphi_{rad},n))$$

$$\varphi_{rad} = \frac{2\pi(rad-1)}{N}$$

$$\alpha(\varphi_{rad},n) = arc\,tan(\frac{Grad_{nC}}{Grad_{nR}})$$

Where $Grad_{nC}$ and $Grad_{nR}$ represent the column and row gradient at image position n, N represent the number of support region lines irradiate from the center pixel(x, y), Bw represents the sliding band width, r represents the poison of band center in the support region line ranging from R_{min} to R_{max} , and $cos(\varphi_{rad} - \alpha(\varphi_{rad}, n))$ represent the angle between the gradient vector at (φ_{rad}, n) and the direction of φ_{rad}.

In bright field, cell membrane is distinct from the background and cytoplasm is not visible, as we can observe in Figure 2 (b). This leads to the $CI(rad,n)$ in SBF filter did not fit the bright field cell area. By eliminating the affection of divergence and convergence in area of cell membrane in bright field, we transform the convergence index in SBF to facilitate it best fit the cell membrane area. In this paper, the TSBF was given by:

$$TSBF(x,y) = \frac{1}{N}\sum_{rad=1}^{N} \max_{R_{min}<r<R_{max}} \left(\frac{1}{Bw+1} \sum_{r-(Bw/2)}^{r+(Bw/2)} (ABS(CI) + \omega * Gv(rad,n)) \right) \quad (4)$$

With

$$ABS(CI) = \|CI(rad,n)\|$$

$$Gv(rad,n) = \sqrt{Grad_{nC}{}^2 + Grad_{nR}{}^2}$$

Where $ABS(CI)$ is the absolute value of the convergence index at pixel(rad,n), this eliminates characteristic of the divergence and convergence at the location of cell membrane, $Grad(rad,n)$ is the gradient value at pixel(rad,n), ω was a weight parameter (we set $\omega = 1$ in this paper as the default value) designed for the image variation on uneven illumination and out of focus. After applying the TSBF filter to insect cells images, results indicated the cell center was associated with the locations of local maximal value.

The collected insect cell image datasets were then filtered by our designed TSBF filter, and results indicated the center of cell was enhanced, as it was depicted in Figure 2 (c). Then a local maximal suppression filter was applied to detect the local maximal value which was the cell center, result was shown in Figure 2 (d) and the arrow depict the position of location of maximal.

B. Cell Detector Evaluation

To evaluate the accuracy of the proposed method, an error rate estimation process was employed [7]. We selected manual counting results as the Ground Truth (GT), and the performance of cell detector was evaluated by the error criterion according to the Eq (5) and Eq (6).

$$ERT = \frac{|DA - GT|}{GT} \quad (5)$$

$$TERT = \frac{ERT}{NT} \quad (6)$$

With

$$GT = \frac{N_{s1} + N_{s2} + N_{s3}}{3}$$

$$DA = \frac{D_{s1} + D_{s2} + D_{s3}}{3}$$

$$N_{si} = \frac{Sample_{i_{sui}} + Sample_{i_{dai}} + Sample_{i_{zhang}}}{3}, \quad i \in \{1,2,3\}$$

Where Error Rate of TSBF (ERT) is the relative error rate at a certain cell density calculated using the TSBF filter compared with manual counting, Total Error Rate of TSBF (TERT) is the average of relative error rate in all cell density calculated by the proposed method, NT is the number of cell samples in different density, GT is the Ground Truth, Sample_i is cell density of a sample from certain time counted by lab collaborator Sui, Dai and Zhang. N_{si} is average number of Sample_i,. For example, after recovering from the liquid nutrition, cell suspension with density of 5×10^5 cells/mL was made by experienced lab collaborator as the starting point, 3 samples was collected each 24th hours until the 216th hours (the 9th days). *Sf*9 insect cells were counted by 3 lab collaborator and the proposed method separately.

IV. Results and Discussion

For the insect cells image dataset, the following parameters were set based on visual inspection directly. For the cell detection, $R_{min} = 8$, $R_{max} = 30$. Regarding the remaining of SBF filter parameter we set $N = 32$, $d = 6$.

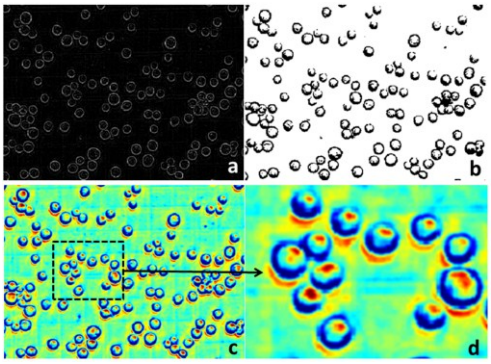

Figure 3. Sf9 cell detection comparison between Laplacian of Gaussian (LoG) method (a), intensity threshold method (b), TSBF method (c)and (d) was a magnification of parts in (c).

Comparison results between the TSBF and traditional image enhancement methods showed an excellent performance of our proposed method in insect cell image enhancement, Figure 3 shows the comparisons between LOG, intensity threshold and TSBF method. Results indicated the TSBF method can detect the insect cells as higher filter resonance value in the center of cell cytoplasm and compared with the other two traditionally methods, which merely detected the cell membrane area in the bright field images.

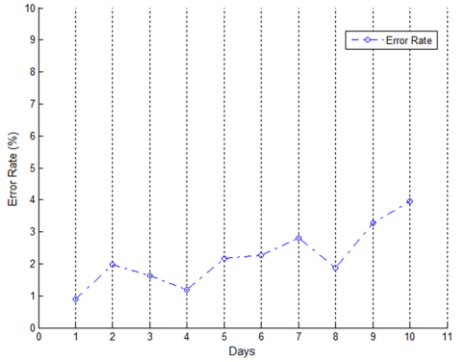

Figure 4. Total Error rate result of TSBF. X axis represents the days; Y axis represents the total error rate (ERT) generated by TSBF method.

We tested our method on insect cells datasets from different period of cultivation. For each sample of insect cells, masks were employed to cover the A1 to A5 region of Neubauer chambers separately in Figure 1, and then we manually calculated each sample by 3 lay collaborators Sui,

Dai and Zhang to create the ground truth for investigating the variation between manual counting and TSBF method.

TERT is an important criterion to evaluate the accuracy of cell detector. The TERT of TSBF method is 2.21%, ranging from 0.89% to 3.97%. Result of ERT each day collected was shown in Figure 4. When insect cells were cultivated using the method of cell suspension, and with the growth of density, cells usually crowed together when they were out of shaker, and some cells still exhibited crowed after injecting into the chamber, which was usually identified as one cell by manual counting but was detected as 2, 3 or more cells by TSBF method. This leads to the total error rate exhibited an up growth manner with insect cells growth. To verify this assumption, we diluted the cell suspension to make sure cells were separated from each other at the 4th and 8th day, results showed a decrease of ERT. Unfortunately, after cell grow into stationary phase, some cells was corrupted for lacking of nutrition, and the TSBF method detected the bigger cell corruption as single cell which lead to the error rate increase, Shown in Figure 4. Fortunately, insect cells in this phase were out of use for experiments, so this defect can be omitted.

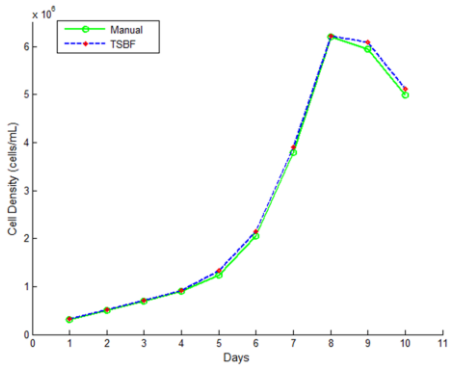

Figure 5. Growth curve of Sf9 insect cell. X axis represent the days; Y axis represent the cell density.

V. CONCLUSION

In this paper, a novel cell counting method based on TSBF was proposed for insect cells in bright field microscope image datasets which was collected by confocal microscopy in BVES protocol. The growth curve produced was consistent with the manual results. In detecting the insect cells, the method exhibited an excellent performance with its accuracy and the average error rate is 2.21% ranging from 0.89% to 3.97% in all datasets.

Finally, it is worth noting that application of this method can clearly benefit for insect cell counting task in the protocol of BEVS. However, uneven illumination produced by microscope was also critical factor influencing identification accuracy. So some illumination correction methods will be studied to improve our method in the future works.

ACKNOWLEDGMENT

This paper was supported by National Nature Science Foundation of China (NSFC) grant No. 61001167, No.61173086 and No.61179009.

REFERENCES

[1] M. Marek, M. M. van Oers, F. F. Devaraj, J. M. Vlak, and O. W. Merten, "Engineering of baculovirus vectors for the manufacture of virion - free biopharmaceuticals," *Biotechnology and bioengineering,* vol. 108, pp. 1056-1067, 2011.

[2] C. D. Helgason and C. L. Miller, *Basic cell culture protocols* vol. 1: Humana Pr Inc, 2005.

[3] M. E. Bracke, T. Boterberg, E. A. Bruyneel, and M. M. Mareel, "Collagen invasion assay," *Methods in molecular medicine,* vol. 58, pp. 81-90, 2001.

[4] D. Demandolx and J. Davoust, "Multiparameter image cytometry: from confocal micrographs to subcellular fluorograms," *Bioimaging,* vol. 5, pp. 159-169, 1997.

[5] N. Malpica, C. Ortiz de Solorzano, J. J. Vaquero, A. Santos, I. Vallcorba, J. M. Garcia-Sagredo, and F. del Pozo, "Applying watershed algorithms to the segmentation of clustered nuclei," *Cytometry,* vol. 28, pp. 289-297, 1997.

[6] A. Nedzved, S. Ablameyko, and I. Pitas, "Morphological segmentation of histology cell images," 2000, pp. 500-503 vol. 1.

[7] M. Usaj, D. Torkar, M. Kanduser, and D. Miklavcic, "Cell counting tool parameters optimization approach for electroporation efficiency determination of attached cells in phase contrast images," *Journal of Microscopy,* vol. 241, pp. 303-314, 2011.

[8] M. R. Lamprecht, D. M. Sabatini, and A. E. Carpenter, "CellProfiler™: free, versatile software for automated biological image analysis," *Biotechniques,* vol. 42, p. 71, 2007.

[9] K. Preston Jr, "Image processing in medical microscopy," 1986, p. 213.

[10] K. Preston, "High-resolution image analysis," *Journal of Histochemistry & Cytochemistry,* vol. 34, p. 67, 1986.

[11] C. Pereira, H. Fernandes, A. Mendonça, and A. Campilho, "Detection of lung nodule candidates in chest radiographs," *Pattern Recognition and Image Analysis,* pp. 170-177, 2007.

[12] C. Pereira, A. Mendonça, and A. Campilho, "Evaluation of contrast enhancement filters for lung nodule detection," *Image Analysis and Recognition,* pp. 878-888, 2007.

[13] P. Quelhas, M. Marcuzzo, A. M. Mendonca, and A. Campilho, "Cell Nuclei and Cytoplasm Joint Segmentation Using the Sliding Band Filter," *IEEE Transactions on Medical Imaging,* vol. 29, pp. 1463-1473, Aug 2010.

[14] W. Hink, D. Thomsen, D. Davidson, A. Meyer, and F. Castellino, "Expression of three recombinant proteins using baculovirus vectors in 23 insect cell lines," *Biotechnology progress,* vol. 7, pp. 9-14, 1991.

[15] R. Gonzalez and R. Woods, "Digital Image Processing–Addison Wesley Publishing Company," ed: USA, 2008.

[16] H. Kobatake and S. Hashimoto, "Convergence index filter for vector fields," *Image Processing, IEEE Transactions on,* vol. 8, pp. 1029-1038, 1999.

[17] J. Wei, Y. Hagihara, and H. Kobatake, "Detection of rounded opacities on chest radiographs using convergence index filter," 1999, pp. 757-761.